JCTC Journal of Chemical Theory and Computation

Article

pubs.acs.org/JCTC

Behavior of the Position−Spread Tensor in Diatomic Systems

Oriana Brea,[†,‡] Muammar El Khatib,[†] Celestino Angeli,*[,§] Gian Luigi Bendazzoli,[¶] Stefano Evangelisti,[†] and Thierry Leininger[†]

[†]Laboratoire de Chimie et Physique Quantiques, Université de Toulouse et CNRS, 118, Route de Narbonne, F-31062 Toulouse Cedex, France

[‡]Departamento de Química, Facultad de Ciencias, Módulo 13, Universidad Autónoma de Madrid, Cantoblanco, 28049 Madrid, Spain

[§]Dipartimento di Scienze Chimiche e Farmaceutiche, Università di Ferrara, Via Borsari 46, I-44121 Ferrara, Italy

[¶]P.A.M. Università di Bologna, Dipartimento di Chimica Industriale "Toso Montanari", Viale Risorgimento 4, I-40136 Bologna, Italy

Supporting Information

ABSTRACT: The behavior of the Position−Spread Tensor ($\mathbf{\Lambda}$) in a series of light diatomic molecules (either neutral or negative ions) is investigated at a Full Configuration Interaction level. This tensor, which is the second moment cumulant of the total position operator, is invariant with respect to molecular translations, while its trace is also rotationally invariant. Moreover, the tensor is additive in the case of noninteracting subsystems and can be seen as an intrinsic property of a molecule. In the present work, it is shown that the longitudinal component of the tensor, $\mathbf{\Lambda}_{\parallel}$, which is small for internuclear distances close to the equilibrium, tends to grow if the bond is stretched. A maximum is reached in the region of the bond breaking, then $\mathbf{\Lambda}_{\parallel}$ decreases and converges toward the isolated-atom value. The degenerate transversal components, $\mathbf{\Lambda}_{\perp}$, on the other hand, usually have a monotonic growth toward the atomic value. The Position Spread is extremely sensitive to reorganization of the molecular wave function, and it becomes larger in the case of an increase of the electron mobility, as illustrated by the neutral-ionic avoided crossing in LiF. For these reasons, the Position Spread can be an extremely useful property that characterizes the nature of the wave function in a molecular system.

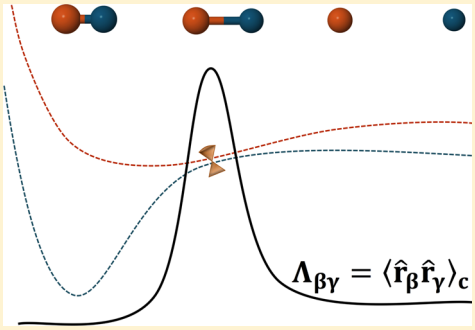

1. INTRODUCTION

The "Localization Tensor" (LT) is a quantity introduced in the context of the theory of Kohn[1] to characterize the electrical conductivity properties. Indeed, in his seminal work, Kohn realized that the most fundamental picture of electrical conductivity is more related to a properly defined delocalization of the wave function than to the simple gap closure. Subsequently, Resta and co-workers, with the introduction of the localization tensor, provided an important tool to give a quantitative formulation of this localization.[2−4] According to their results, one of the key properties of this quantity is the following: it diverges in the thermodynamic limit for a conductor, while remaining finite for an insulator. A remarkable sum rule connecting explicitly the electrical resistivity and the localization tensor was later given by Souza, Wilkens, and Martin[5] (also see ref 6). The LT has been considered as an indicator of the square of the exchange-correlation lengths in the electronic distribution, that is of the extension of the influence of one electron on the other electrons.[7] We have recently applied the LT formalism to the study of low-dimensional systems (linear chains, graphene nanoislands), either at ab initio[8−12] or tight-binding level[13−16] (also see ref 17). A remarkable study of the localization tensor for small molecular systems has been recently reported by Ángyán.[18]

The interest related to the application of the LT to molecular systems is 2-fold: first, one can study the insulator/conductor properties as a function of the size of a homologous series with the aim to clarify the main molecular features affecting these properties. Such an approach is relevant, for instance, in the field of molecular electronics, where the focus is on the possibility to use the molecules as building blocks in the fabrication of the next generation electronic devices. More generally, the LT is an interesting quantity for the systems that are in the intermediate region between "chemistry" and "solid-state physics"—the subject of nanotechnology. A second interest for the applications of the LT to molecular systems is more strictly related to the electronic structure of the molecules. Indeed, this quantity allows to identify, besides the insulator/conductor nature, intriguing properties of the electronic distribution with a connection to the chemical description of the molecular architecture.

As said, the LT has been introduced to identify the electrical conductivity properties in solid-state physics, and, for this reason, it is a "per electron" quantity. In molecular studies, while this choice maintains its interest for the first application field described above, for its use in the analysis of the molecular wave function, the full quantity (not divided by the number of electrons) seems more appropriate. For this reason, we introduce the Total Position−Spread (TPS) tensor ($\mathbf{\Lambda}$),

Received: May 31, 2013
Published: November 5, 2013

Table 1. Dissociation Energies (eV) and Equilibrium Distances (bohr) for the Diatomic Molecules Considered in This Study, And Their Basis Set

		This Work		Reference Data			
molecule	basis set	R_e (bohr)	E_{dis} (eV)	R_e (bohr)	ref	E_{dis} (eV)	ref
H_2^+	(7*s*3*p*3*d*3*f*)	1.99	2.7896	1.99	40	2.6507	41
H_2	(7*s*3*p*3*d*3*f*)	1.40	4.7279	1.40	42	4.7474	42
Li_2	(7*s*6*p*4*d*3*f*)	5.10	1.0421	5.05	43	1.0260	43
N_2	(3*s*2*p*)	2.15	6.9511	2.07	44	9.7797	44
F_2	(3*s*2*p*)	2.96	0.8209	2.67	45	1.6261	45
LiF 1 $^1\Sigma$	(3*s*2*p*/3*s*2*p*)	3.10	5.2604	2.96	46	5.9625	46
He_2	(7*s*4*p*3*d*)	5.65	0.0008	5.61	47	0.0009	47
HeH^-	(7*s*4*p*3*d*/6*s*4*p*3*d*)	11.50	0.0001	11.50	48	0.0004	37
Be_2	(7*s*7*p*4*d*3*f*)	4.75	0.0906	4.63	49	0.0979	49
BeH^-	(7*s*7*p*4*d*3*f*/6*s*4*p*3*d*)	2.75	1.9730	2.67	50	2.2000	50

which is defined as the second moment cumulant of the total electron position operator. In this work, the behavior of $\mathbf{\Lambda}$ for a series of diatomic molecules and ions has been investigated, as a function of the internuclear distance R. The results of the present study can be summarized as follows. Let us first consider the longitudinal component of the tensor, $\mathbf{\Lambda}_{\parallel}$, the one in the direction of the internuclear axis, z. As a general trend, one observes that, close to the equilibrium distance, $\mathbf{\Lambda}_{\parallel}(R)$ is a growing function of R. $\mathbf{\Lambda}_{\parallel}(R)$ generally reaches a maximum in the region where the bond is broken, and then it becomes a decreasing function of R. For very large values of R, $\mathbf{\Lambda}_{\parallel}(R)$ becomes a constant, given by the sum of the atomic values. The peak in the region of the bond breaking is often very pronounced. The two perpendicular components, denoted from now on as $\mathbf{\Lambda}_{\perp}(R)$ ($\mathbf{\Lambda}_{xx}(R)$ and $\mathbf{\Lambda}_{yy}(R)$), are obviously degenerate for symmetry reasons in isolated diatomic molecules. Their behavior generally is less spectacular than the parallel one, and their values are often growing monotonically to the asymptotic limit in a smooth way.

The remaining of the paper is organized as follows: in Section 2, the definition of the TPS tensor is shortly recalled, the computational details are described in Section 3, the numerical values of the TPS tensor are reported and discussed in Section 4, and Section 5 contains some final considerations.

2. THE TOTAL POSITION−SPREAD TENSOR

The TPS tensor, indicated by $\mathbf{\Lambda}$, is defined as the second moment cumulant of the total electron position operator. As detailed in ref 11, one considers the position operator and its tensorial square:

$$\hat{r}_\beta = \sum_{p=1}^{n} \hat{\beta}(p) \tag{1}$$

$$\hat{r}_\beta \hat{r}_\gamma = \sum_{p,q=1}^{n} \hat{\beta}(p)\hat{\gamma}(q) \tag{2}$$

where the sums run over the electrons (n is the total number of electrons) and β and γ represent one of the Cartesian coordinates (x, y, and z).

The cumulant of the quadratic fluctuation of the position is

$$\langle \hat{r}_\beta \hat{r}_\gamma \rangle_c = \langle \Psi | \hat{r}_\beta \hat{r}_\gamma | \Psi \rangle - \langle \Psi | \hat{r}_\beta | \Psi \rangle \langle \Psi | \hat{r}_\gamma | \Psi \rangle \tag{3}$$

Finally, the localization tensor is defined as

$$\lambda_{\beta\gamma}{}^2 = \frac{\langle \hat{r}_\beta \hat{r}_\gamma \rangle_c}{n} \tag{4}$$

The expression "localization tensor" is somehow misleading, as already pointed out by Ángyán,[19] since very mobile electrons are associated with large values of the tensor. Moreover, as stated in the Introduction, in a molecular context, we believe that the more interesting quantity is not the *per electron* spread, but rather the global value. We stress this fact by denoting Total Position Spread this quantity, with components $\mathbf{\Lambda}_{\beta\gamma} = \langle \hat{r}_\beta \hat{r}_\gamma \rangle_c$. The reason for the interest in the global quantity is because only the TPS shows a size consistency property: the TPS of noninteracting fragments is given by the sum of the TPS of the individual fragments, while, obviously, the LT does not have this property. This is true for each individual component of the tensor and, of course, for the trace that becomes a rotational invariant. As a consequence, the trace of the TPS is an additive and rotationally invariant quantity associated with a molecular system.

3. COMPUTATIONAL DETAILS

In the present work, we investigate at Full Configuration Interaction (FCI) level the behavior of the ground-state TPS tensor for a series of diatomic systems, belonging to the first two periods of the periodic table: homonuclear diatomic molecules (H_2, He_2, Li_2, Be_2, N_2, F_2) and one heteroatomic molecule that shows an ionic-neutral avoided crossing (LiF). The ionic systems HeH^- and BeH^- were also considered. All chosen systems have closed-shell singlet ground states: $^1\Sigma_g^+$ for homonuclear and $^1\Sigma^+$ for heteroatomic systems. Open-shell systems will be the subject of forthcoming investigations.

We used the ANO basis sets optimized by Roos and coworkers,[20] by adopting contractions of different qualities. In particular, we employed the following contractions for the diatomic molecules that have been considered in this study: H_2, 7*s*3*p*3*d*3*f*; Li_2, 7*s*6*p*4*d*3*f*; He_2, 7*s*4*p*3*d*; HeH^-, 7*s*4*p*3*d* − 6*s*4*p*3*d*; Be_2, 7*s*7*p*4*d*3*f*; BeH^-, 7*s*7*p*4*d*3*f* − 6*s*4*p*3*d*; LiF, N_2 and F_2, 3*s*2*p*. The choice of the basis set is limited by the size of the FCI space, which shows a factorial growth as a function of the number of electrons and the size of the basis set. The initial Hartree−Fock calculations were performed using the computational ab initio Quantum-Chemistry package DALTON.[21,22] The atomic one- and two-electron integrals then were transformed to the molecular basis set, using the Ferrara code.[23] Finally, the Full-CI calculations were performed using our FCI algorithm,[24−26] implemented in the NEPTUNUS

code[27] and interfaced to the previous codes using the common data formats Q5Cost.[28−30]

The 1*s* electrons were kept frozen at the Hartree−Fock level for all atoms but hydrogen and helium. The contribution of these frozen electrons to the TPS tensor was taken into account through a generalization of the formalism discussed in Section 2. However, its value is extremely small, and our preliminary investigations show that the effect of including (or not including) the dynamic electron correlation for these electrons has a negligible effect.

4. RESULTS AND DISCUSSION

In Table 1, the equilibrium distance and the dissociation energy obtained at FCI level are compared to the experimental results (when available). For all systems here considered, the ground-state potential energy curve is reported in the Supporting Information. In the case of the ions BeH^- and HeH^- (for which, to the best of our knowledge, there is no experimental data), we have compared our results with those obtained at FCI level with a larger basis set. From the values reported in Table 1, it is apparent that all results are of a reasonable quality, except for the systems involving nitrogen (N_2) or fluorine (F_2 and LiF), for which the dissociation energy is seriously underestimated. This fact, in view of the small basis set that we were forced to use in order to treat these molecules at FCI level, is certainly not surprising. We consider now in detail the behavior of the TPS tensor for the different systems.

4.1. Covalent and Ionic Systems. Here, we examine the behavior of systems having strong covalent or ionic bonds. The considered systems are the covalent species H_2, Li_2, N_2, and F_2, and the strongly ionic molecule LiF.

In the case of a singlet covalent bond, the equilibrium wave function is known to be a mixture of neutral and ionic forms. The nature of the ground state of the prototype of all molecules showing covalent bonds, the H_2 molecule, has been analyzed in detail in terms of Orthogonal Valence Bond (OVB) structures in ref 31, and the influence of the relative weight of the ionic and neutral structures in the ground state wave function on the LT has been described in ref 11. In summary, starting from the equilibrium geometry, the weight of the ionic forms slightly decreases by increasing the interatomic distance. However, for these structures, the value of $\Lambda_\parallel$ quickly grows with R. As a result, the value of $\Lambda_\parallel$ computed for the full ground-state wave function increases as a function of R. This picture is valid in the region of the bond. When the bond is broken, however, we have a dramatic change in the nature of the wave function, and the weight of the ionic forms quickly goes to zero as R is increased. The contribution of these forms becomes negligible, and the value of $\Lambda_\parallel$ goes quickly to the asymptotic atomic limit.

For the simple case of H_2 in the minimal basis set, the longitudinal component of the TPS computed for the approximate UHF wave function shows an interesting behavior and allows one to discuss the dependence of $\Lambda_\parallel$ on R from a slightly different point of view. Indeed, for R smaller than the Coulson−Fischer point (computed to be at 2.287 bohr in the 1*s* basis), the UHF wave function coincides with the RHF wave function; therefore, it is a superposition of the neutral and ionic OVB forms with equal weight. In this case, $\Lambda_\parallel$ is a growing function of R (scaling as R^2). On the other hand, for R larger than the Coulson−Fischer point, the UHF wave function becomes the broken-symmetry, spin-contaminated, solution for which $\Lambda_\parallel$ slowly approaches the value of the neutral OVB structure (it converges to this value for $R \to \infty$). Therefore, starting from R_e and increasing R, $\Lambda_\parallel$ shows a marked increase up to $R \simeq 2.3$ bohr and then a decrease to the sum of the atomic values. This behavior has been confirmed computing $\Lambda_\parallel$ as a function of R for the UHF wave function with the STO12G basis set used in ref 11 (see the Supporting Information). Obviously, the UHF wave function is only a rough approximation to the FCI wave function and the maximum of $\Lambda_\parallel$ observed in the minimal basis set at the FCI level is at a slightly different value of R (R = 2.76 bohr, see ref 11), but the simple picture offered by the UHF description allows to identify the main features of $\Lambda_\parallel$.

This scheme can be rationalized and fully understood by other simple qualitative considerations (see the Appendix). In fact, as can be easily shown, even at the Hückel level, two electrons in two localized orbitals coupled to form a singlet wave function give a vanishing value for $\Lambda_\parallel$. The same result is also obtained if the two electrons occupy the same localized orbital. In contrast, when the wave function is a combination of the two ionic forms obtained by placing the two electrons in one of the two local orbitals, the value of $\Lambda_\parallel$ is nonzero. Moreover, for a fixed mixing between the two localized ionic forms, the TPS grows as the square of the distance between the two centers.

Let us consider now the case of an "ionic" bond, again by using this simple approach. In such a case, one generally has a mixture between an ionic and a neutral structure, their relative weight being a function of the interatomic distance. Usually, at the equilibrium distance, the ionic structure dominates in the ground state wave function, while at dissociation, it is the neutral structure that describes the ground state (no diatomic molecule dissociates to a pair of ionic atoms). Therefore, there is a distance where the two states undergo an avoided crossing and, in the crossing region, the wave function is a mixture of ionic and neutral forms.

Of course, things become more complicated at the ab initio level, since, in this case, the atomic contributions also must be taken into account (these terms are neglected in the simple approach described above). However, these intra-atomic contributions tend to be significantly smaller than the interatomic ones, so the general picture obtained at Hückel level is still valid when the complete Hamiltonian is considered.

These considerations are confirmed by the calculations reported in the present work. For all covalent systems, a similar behavior is observed and hereafter briefly described. The perpendicular value, $\Lambda_\perp$, is usually smaller for the molecule at the equilibrium geometry than for the dissociated atoms. This behavior is due to the increased nuclear effective charge experienced by the electrons at short internuclear distances (two nuclei instead of only one), which leads to a spatial contraction of the orbitals in the directions orthogonal to the internuclear axis. This, in turn, induces a reduction of the $\perp$ component of the TPS tensor. The parallel component, $\Lambda_\parallel$, starts at small values of R from a value smaller than the asymptotic limit (for the same reason reported for $\Lambda_\perp$) and shows a quick growth by increasing R. Close to the equilibrium distance, the value becomes close to the asymptotic limit but it keeps growing. At a distance close to the bond-breaking distance, $\Lambda_\parallel$ has a maximum and then it falls down to the isolated-atom limit. One can assume, in a rather conventional way, the bond-breaking distance to be the distance at which the energy slope has a maximum, or, equivalently, where the second derivative of the energy, with respect to the internuclear distance, becomes zero. From Table 2 it is apparent that the

Table 2. Bond-Breaking Distance (Bohr) Computed as the Distance at Which the Second Derivative of the Energy, with Respect to the Internuclear Distance, Vanishes

molecule	R
H_2	2.14
Li_2	6.90
N_2	2.68
F_2	3.46
LiF	4.27
He_2	6.36
HeH^-	13.58
Be_2	5.21
BeH^-	3.49

position of the TPS maximum is often close to the bond-breaking distance, although it is generally slightly larger. The system where there is a charge transfer from one atom to the other one as a function of the distance (LiF, BeH^-) does not follow this pattern, since, in this case, the TPS maximum occurs at the distance of the charge jump.

This picture explains the behavior of $\mathbf{\Lambda}$ in the case of covalent bonds, such as H_2, Li_2, and N_2, and it is illustrated in Figures 1−3. The F_2 molecule (see Figure 4) differs from the

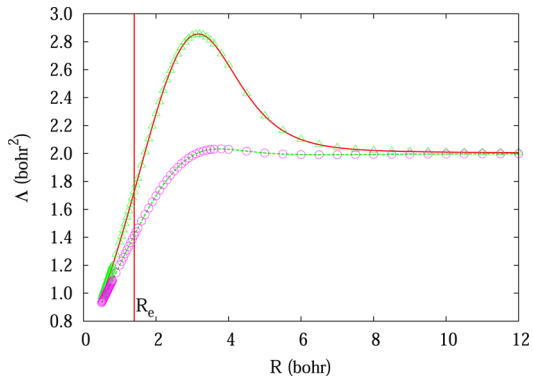

Figure 1. Total Position Spread computed for the $^1\Sigma_g^+$ ground state of the hydrogen dimer at Full CI (FCI) level of theory: $\Lambda_\parallel$, which is denoted by the red solid line and triangles, and $\Lambda_\perp$, which is denoted by the green dashed line and circles. The equilibrium geometry is indicated by a vertical line.

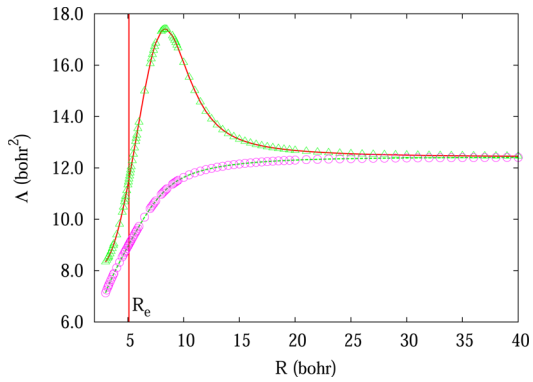

Figure 2. Total Position Spread computed for the $^1\Sigma_g^+$ ground state of the lithium dimer at Full CI (FCI) level of theory: $\Lambda_\parallel$, which is denoted by the red solid line and triangles, and $\Lambda_\perp$, which is denoted by the green dashed line and circles. The equilibrium geometry is indicated with a vertical line.

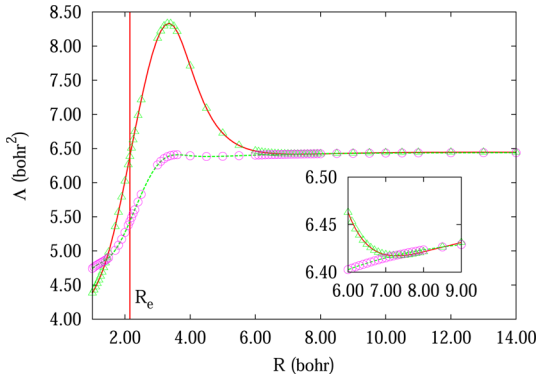

Figure 3. Total Position Spread computed for the $^1\Sigma_g^+$ ground state of the nitrogen dimer at Full CI (FCI) level of theory: $\Lambda_\parallel$, which is denoted by the red solid line and triangles, and $\Lambda_\perp$, which is denoted by the green dashed line and circles. In the inset zoom, the local minimum of Λ is reported. The equilibrium geometry is indicated with a vertical line.

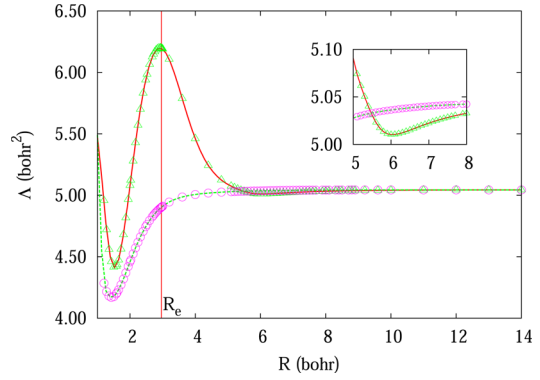

Figure 4. Total Position Spread computed for the $^1\Sigma_g^+$ ground state of the fluorine dimer at Full CI (FCI) level of theory: $\Lambda_\parallel$, which is denoted by the red solid line and triangles, and $\Lambda_\perp$, which is denoted by the green dashed line and circles. In the inset zoom, the local minimum of Λ is reported. The equilibrium geometry is indicated with a vertical line.

above scenario, since the maximum is reached for values of R that are very close to the equilibrium distance. This result is a manifestation of the peculiar nature of the bond in this molecule, as it has been pointed out in valence bond and electron localization function studies,[32,33] where it has been shown that the fluctuation of the electron pair density play an important role for the bond formation, so that it has been termed *charge-shift bonds*. Moreover, after its maximum value, $\Lambda_\parallel$ has a very shallow minimum before reaching its asymptotic value from below. Actually, a similar behavior is also seen in the nitrogen dimer, although the depth of the minimum, in this case, is much smaller.

In order to identify the origin of the appearance of this minimum in F_2 and N_2, we have reconsidered the analytical OVB approach applied to H_2 with the minimal 1*s* basis set, which has been fully developed in refs 11 and 31. In order to simulate different bond situations, the off-diagonal element of the Hamiltonian matrix between the neutral and the ionic Σ_g components (eq 20 in ref 31) has been scaled by a factor k. For $k < 1$, after the diagonalization of the 2×2 Hamiltonian matrix, the weight of the ionic OVB structure in the ground state is lower than for $k = 1$ (corresponding to the exact treatment of H_2) for all geometries. This effect is particularly intense in the

dx.doi.org/10.1021/ct400453b | J. Chem. Theory Comput. 2013, 9, 5286−5295

region between the equilibrium geometry and the bond-breaking geometry, where the smaller k is, the quicker the decrease of the weight of the ionic structures with R. Such a modification has a marked effect on the qualitative dependence of $\Lambda_{\parallel}$ on R, as it is apparent from Figure 5, where $\Lambda_{\parallel}$ is

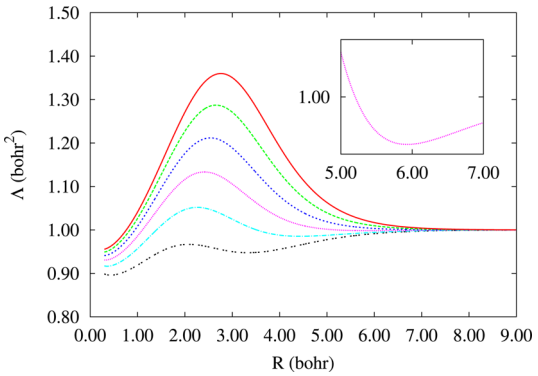

Figure 5. Longitudinal Total Position Spread component, $\Lambda_{\parallel}$, computed for the $^1\Sigma_g^+$ ground state of the hydrogen dimer at the minimal basis OVB level of theory with a scaling by a factor k of the off-diagonal element of the Hamiltonian matrix between the neutral and the ionic Σ_g OVB components. k = 1 for the top curve (red solid line), while k = 0.5 for the bottom curve (black dashed line). The other curves are reported for intermediate values of k with steps of 0.1. In the inset enlargement, the local minimum of $\Lambda_{\parallel}$ is reported for the k = 0.7 case (pink dashed curve).

reported as a function of R for k = 0.5, 0.6, 0.7, 0.8, 0.9, 1.0. One notes that the maximum observed for k = 1 is lowered and shifted at smaller R when k is reduced. Moreover, a minimum appears at long R values for k = 0.5, 0.6, 0.7 (the inset of Figure 5 reports a zoom in the minimum region for k = 0.7).

These results suggest that the minimum observed for N_2 and F_2 (see Figures 3 and 4) can be due to a lower weight of the ionic OVB component in the ground state of these molecules, with respect to the other dimers considered here. The same argument could also explain the fact that the maximum of $\Lambda_{\parallel}$ in F_2 is at R close to the equilibrium internuclear distance.

The ionic system LiF has a particularly interesting behavior. The nature of the two relevant states in this system, as in all molecules of the type MX, where M is an alkali metal and X is a halogen, can be understood in terms of two diabatic states: one dissociating to the neutral M + X atomic limit, and the other one to the ionic $M^+ + X^-$ limit (which is, for all diatomic molecules, always higher in energy than the M + X asymptote). For a complete discussion, the reader is referred to ref 34. Similarly to what is observed for H_2,[35] the neutral state is dissociative (no bond). In contrast, the ionic diabatic state is strongly bound, due to the strong Coulombic interaction. At short internuclear distances, the ionic diabatic state is lower in energy than the neutral one, as a result of the low value of the ionization potential of M and of the large value of the electron affinity of X, which makes the energy of the $M^+ + X^-$ atomic limit not too high in energy, with respect to the M + X one. Therefore, the two diabatic energies become equal at a distance larger than the equilibrium geometry, in the case of LiF for a value of R of ∼11.10 bohr, and the system shows an avoided crossing between the two states (see Figure 6). This behavior has been discussed in detail in a paper by Bauschlicher and Langhoff.[36] The two diabatic states are described, at a first approximation, by an ionic determinant (the ionic state), and a

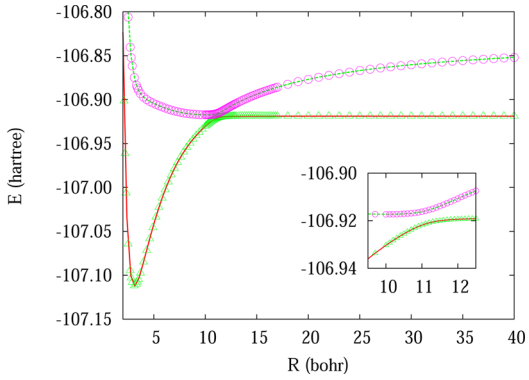

Figure 6. Potential energy curve of LiF for the $^1\Sigma^+$ ground state (red solid line and triangles) and first excited state (green dashed line and circles) at Full CI (FCI) level of theory. In the enlargement shown as an inset, the avoiding crossing region is reported.

singlet combination of purely neutral determinants. The dependence of $\Lambda_{\perp}$ on R is reported in Figure 7 for the two

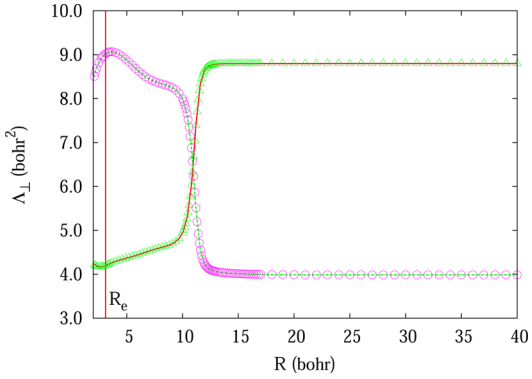

Figure 7. Total Position Spread ($\Lambda_{\perp}$ component), computed for the $^1\Sigma^+$ ground state (red solid line and triangles) and first excited state (green dashed line and circles) of the lithium fluorine (LiF) molecule at Full CI (FCI) level of theory.

states. One notes that, as intuitively expected, $\Lambda_{\perp}$ changes suddenly passing the crossing region (for the ground state from the "ionic value" before the crossing, to the "neutral value" after the crossing and vice versa for the excited state). In contrast, the behavior of $\Lambda_{\parallel}$ (reported in Figure 8) is more complex. As

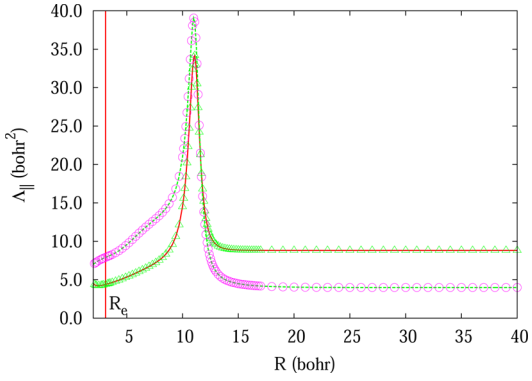

Figure 8. Total Position Spread ($\Lambda_{\parallel}$ component), computed for the $^1\Sigma^+$ ground state (red solid line and triangles) and first excited state (green dashed line and circles) of the lithium fluorine (LiF) molecule at Full CI level of theory.

dx.doi.org/10.1021/ct400453b | J. Chem. Theory Comput. 2013, 9, 5286−5295

described in the Appendix, the ionic and neutral wave functions, taken separately, have a strictly zero longitudinal TPS at the Hückel level. When they are combined, however, their TPS is equal to the product of the squares of the coefficients. From Figure 8, in fact, one sees that the TPS of the two states remains close to the asymptotic values for all R values except in the avoided-cross region. Close to the cross region, near to 11 bohr with the employed basis set, the Hückel value is expected to have a maximum of $R^2/4$, which amounts to ∼30 bohr^2. This is in very good agreement with the increase of the TPSs in this region, that is comprised between 25 and 35 bohr^2 for the ground state and the excited state, respectively.

4.2. Molecular Anions and Weakly Bonded Systems. We will examine now the behavior of systems whose bonds are weak or very weak: the neutral dimers of helium and beryllium (He_2 and Be_2), and the anions that these atoms form by combination with the hydrogen anion (HeH^- and BeH^-).

Among these species, Be_2 has a TPS that is very much alike that those of the previously considered covalent dimers (see Figure 9). This confirms the fact that, although very weak, the bond in this molecule has essentially a covalent nature.

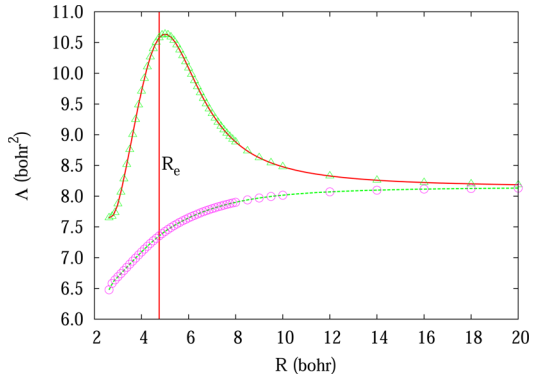

Figure 9. Total Position Spread ($\Lambda_\parallel$, red solid line and triangles; $\Lambda_\perp$ green dashed line and circles), computed for the $^1\Sigma_g^+$ ground state of Be_2 at Full CI (FCI) level of theory. The equilibrium geometry is indicated with a vertical line.

The helium dimer, on the other hand, has a marked TPS peak at very short interatomic distance (see Figure 10). This can be explained by the fact that its value, in the united-atom limit, must converge to that of the beryllium atom. This is

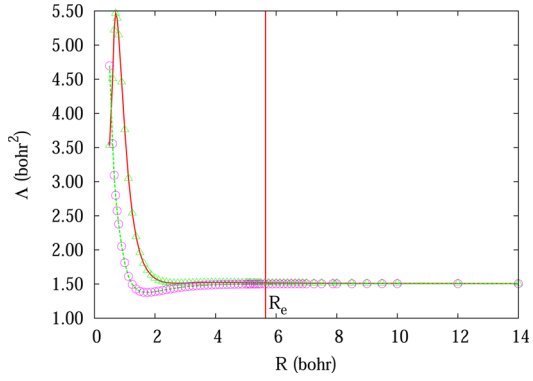

Figure 10. Total Position Spread ($\Lambda_\parallel$, red solid line and triangles; $\Lambda_\perp$ green dashed line and circles), computed for the $^1\Sigma_g^+$ ground state of the helium dimer at Full CI (FCI) level of theory. The equilibrium geometry is indicated with a vertical line.

indeed the case, since the short-distance value of the He_2 system oscillates between 4 and 5.5 bohr^2, while the corresponding value for a beryllium atom is ∼5 bohr^2. The oscillations shown by the helium-dimer values (the longitudinal component in a particular way) at very short distance are most likely due to changes in the configuration structure of the wave function. In view of the fact that our basis set is certainly not suitable for a short distance description of the system (because of the lack of very concentrated atomic orbitals (AOs)), we did not carry this analysis at a deeper level.

As far as the two ions are concerned, their behavior is rather different from those of the neutral systems. In the case of HeH^- system, we have an extremely weakly bonded system. The interactions are of the charge-induced dipole type, and the minimum well is only a few cm^{-1} deep.[37] The TPS values become very high at short internuclear distances, where they converge to the united-atom limit (see Figure 11). More

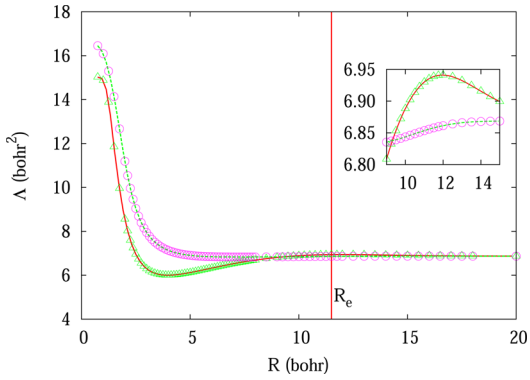

Figure 11. Total Position Spread ($\Lambda_\parallel$, red solid line and triangles; $\Lambda_\perp$ green dashed line and circles), computed for the $^1\Sigma^+$ ground state of HeH^- at Full CI (FCI) level of theory. In the enlargement shown as an inset, the local maximum of the Total Position Spread $\mathbf{\Lambda}$ is reported. The equilibrium geometry is indicated with a vertical line.

interestingly, there is a maximum of $\Lambda_\parallel$ in the region of the energy minimum, whose depth is much more pronounced than the energy variation. Once again, it is clear that the TPS tensor is very sensitive to variation in the wave function structure that has only a tiny effect on the system energy. BeH^- is a hypothetical system having a covalent nature at short distance.[38] The $\Lambda_\parallel$ component (see Figure 12) has a pronounced maximum in the region where the wave function changes its nature, while the $\Lambda_\perp$ component has a minimum in the same region. At the equilibrium distance, both components have values similar to the asymptotic ones, and they become very large for shorter distances.

4.3. The Long-Distance Behavior of the TPS Tensor. As discussed in Section 2, the TPS tensor is a quantity that is additive for noninteracting systems. The trace of the TPS tensor is invariant under rotations of the coordinate axes, and therefore it is a scalar quantity characterizing the system as a whole. Because of the symmetry of the systems here considered, the component along the internuclear axis, $\Lambda_\parallel$, and the two degenerate components orthogonal to this axis, $\Lambda_\perp$, are additive quantities in the case of noninteracting systems. For this reason, in Table 3, we compared the value of $\Lambda_\parallel$ computed at an internuclear distance of 50 bohr (40 bohr for LiF, as discussed later) with the sum of the atomic values. It should be noticed that in the case of the F atom, a symmetry-broken solution must be considered, in order to have a

dx.doi.org/10.1021/ct400453b | J. Chem. Theory Comput. 2013, 9, 5286−5295

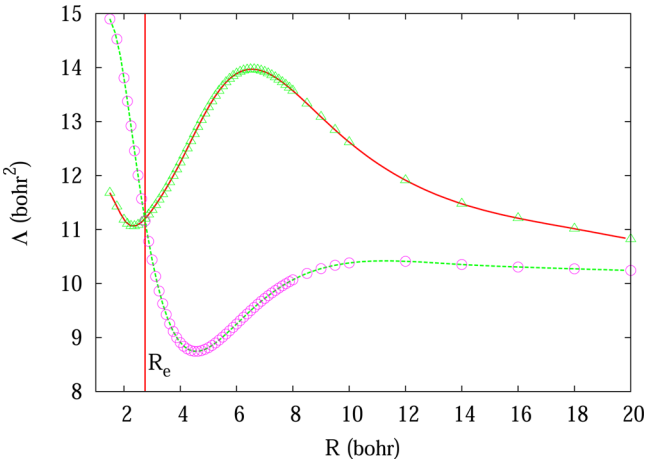

Figure 12. Total Position Spread ($\Lambda_{\parallel}$, red solid line and triangles; $\Lambda_{\perp}$, green dashed line and circles), computed for the $^1\Sigma^+$ ground state of BeH^- at Full CI (FCI) level of theory. The equilibrium geometry is indicated with a vertical line.

Table 3. Total Position Spread (bohr²) Values for the Diatomic Molecules Close to the Dissociation Limit (50 bohr) Except for LiF (40 bohr), Compared to the Sum of Their Corresponding Values for the Isolated Atoms

	Value at Dissociation (50 bohr)		Isolated Atoms (Sum of the Atomic Values)	
molecule	$\Lambda_{\parallel}$	$\Lambda_{\perp}$	$\Lambda_{\parallel}$	$\Lambda_{\perp}$
H_2	2.000742	2.000639	2.000668	2.000668
Li_2	12.439117	12.415638	12.423086	12.423086
N_2	6.441467	6.441315	6.440920	6.440920
F_2	5.050114	5.040229	5.050058	5.040210
LiF ($1^1\Sigma$)	8.805411	8.799939	8.804686	8.799762
LiF ($2^1\Sigma$)	3.986952	3.985769	3.986199	3.986199
He_2	1.506416	1.506392	1.506400	1.506400
HeH^-	6.870093	6.869880	6.869950	6.869950
Be_2	8.152292	8.148845	8.149992	8.149992
BeH^-	10.193261	10.191089	10.191746	10.191746

situation that is comparable with the $D_{\infty h}$ and $C_{\infty v}$ values of the F_2 and LiF molecules, respectively. As an example, one can see in Table 3 that the molecular values of $\Lambda_{\parallel}$ for F_2 at a distance of 50 bohr is 5.050114 bohr², while the sum of the atomic values is 5.050058 bohr² with an absolute percent difference of 5.6×10^{-3}%. It is worth noticing that the energies have a much faster convergence to their asymptotic values, since, at a distance of 50 bohr, the percent difference for the energy is 7.5×10^{-6}% for F_2, compared with the sum of the isolated atoms.

For the sake of comparison, we also reported the values of $\mathbf{\Lambda}$ for the isolated atoms in Table 4. All the values are isotropic, with the exception of fluorine, whose $\Lambda_{\parallel}$ component (one electron in the $2p_z$ orbital) is slightly larger than the $\Lambda_{\perp}$ component (two electrons in the $2p_x$ and $2p_y$ orbitals). This tiny difference is probably due to a compensation between the size of the orbitals and their occupation numbers. We also notice the very large values for Li and, even larger, H^-, and the relatively small increase in Λ in going from F to F^-.

We have already discussed the ionic−covalent avoided crossing of LiF, that occurs at ∼11 bohr. At much larger distances, the LiF ionic energy curve undergoes further, and much more complex, avoided crossings. This is because, at a very large distance (∼43 bohr with the present basis set), the

Table 4. Isolated-Atom Values of the Total Position Spread (bohr²)[a]

atom	Λ
H	1.000334
H^-	6.116750
He	0.753200
Li(7*s*6*p*4*d*3*f*)	6.211543
Li(3*s*2*p*)	6.279657
Li^+(3*s*2*p*)	0.297617
Be	4.074996
N	3.220460
F($\Lambda_{\parallel}$)	2.525029
F($\Lambda_{\perp}$)	2.520105
F^-	3.688582

[a]All values are isotropic with the exception of F, for which the $\Lambda_{\parallel}$ (in the *z* direction) is different from $\Lambda_{\perp}$ (*x* and *y* directions).

energy of the ionic $Li(1s^2)^+ + F(1s^22s^22p^6)^-$ pair becomes degenerate with the neutral pair $Li(1s^22p^1) + F(1s^22s^22p^5)$. The latter gives rise to three highly degenerate singlet states (two of which are exactly degenerate) having a $^1\Sigma^+$ symmetry. These states are obtained by singlet combinations of pairs of determinants having the singly occupied 2*p* orbitals in Li and F of the same type, either *x*, or *y*, or *z*. Therefore, the ionic state undergoes avoided crossings with a bunch of three neutral states, and the behavior of the TPS tensor becomes complicated in the regions of the crossings. Since the study of these crossings is well beyond the scope of the present paper, we are not going to discuss further this aspect. For this reason, the $2^1\Sigma^+$ values reported in Table 3 in the case of LiF were computed at a distance of 40 bohr rather than 50 bohr, where the state having a ionic character is no longer the second $^1\Sigma^+$ state.

5. CONCLUSIONS

The results presented in this work confirm the fact that the TPS tensor is a powerful indicator of the electronic rearrangements in a molecular wave function. Indeed, when a bond is stretched from its equilibrium distance, the longitudinal component of the TPS tensor increases rapidly. The extension of the mutual influence of the electrons keeps increasing, until the bond is broken and then there is a sudden drop-off to the sum of the values found for the two noninteracting atoms. One can therefore conclude that, in the region where the bond is in formation (for *R* between R_e and the distance where the bond is broken), it is characterized by a relatively large extension of the mutual influence of the electrons, while outside this region such influence is more "short range". This is true for diatomic systems, but preliminary results show its usefulness also for more-complex molecular architectures.

Besides the description of the nature of the chemical bond, another interesting possibility concerns the application of this technique to the study of mixed-valence systems. In this case, the TPS tensor is able to describe the delocalized nature of the mobile electrons (or holes) during the transfer process. Together with the mean value of the position operator, this gives an interesting description of the transfer mechanism.

With the aim to apply the strategy here reported to larger systems, we are currently working on the implementation of the algorithm in the MOLPRO code,[39] in particular for the case of CAS-SCF wave functions. This will open a wider possibility of application, since the number of systems that can be treated at

Full CI (FCI) level is rather limited (however, one should stress the fact that rather large CAS-SCF spaces can be treated by using a FCI formalism, if the orbitals are preliminary computed by a general code, and the inactive orbitals are frozen).

APPENDIX

In this Appendix, the analytic expression of the TPS tensor is discussed for the case of a two-electron two-center system having point-like orbitals. This simple model is useful in order to understand the behavior of the TPS in the diatomic molecules considered in this article. Let us consider two centers, A and B, placed at a distance R, with χ_A and χ_B indicating the two point-like orbitals located in the centers A and B, respectively.

The total position operator, $\hat{Z}$ (z being the internuclear axis), is given by

$$\hat{Z} = \hat{z}(1) + \hat{z}(2) \tag{5}$$

where indexes 1 and 2 label electron coordinates. This gives, for its square, the expression

$$\begin{aligned}\hat{Z}^2 &= [\hat{z}(1) + \hat{z}(2)]^2 \\ &= \hat{z}(1)^2 + \hat{z}(2)^2 + \hat{z}(1)\hat{z}(2) + \hat{z}(2)\hat{z}(1)\end{aligned} \tag{6}$$

The first two terms in the last sum correspond to the one-electron part of the operator, $\hat{Z}_m^2$, while the last two terms constitute the two-electron part of the operator, $\hat{Z}_b^2$:

$$\hat{Z}_m^{\,2} = \hat{z}(1)^2 + \hat{z}(2)^2 \tag{7}$$

and

$$\hat{Z}_b^{\,2} = \hat{z}(1)\hat{z}(2) + \hat{z}(2)\hat{z}(1) \tag{8}$$

The TPS tensor is given by the expression

$$\Lambda_{zz} = \langle \hat{Z}^2 \rangle - \langle \hat{Z} \rangle^2 = \langle \hat{Z}_m^{\,2} \rangle + \langle \hat{Z}_b^{\,2} \rangle - \langle \hat{Z} \rangle^2 \tag{9}$$

Notice that $\mathbf{\Lambda}$ is invariant with respect to a translation of the coordinate origin, although the different terms separately are not. This fact can be used to simplify the calculation of the tensor. For instance, if the system has a center of symmetry, the mean value $\langle \hat{Z} \rangle^2$ will be zero if the coordinate origin is chosen to be in the center of symmetry of the system.

We consider first the H_2^+ ion, for which the two relevant wave functions are (only the spatial part is reported):

$$|^2\Psi_g\rangle = \frac{\chi_A(1) + \chi_B(1)}{\sqrt{2}} \quad \text{(doublet } g\text{)} \tag{10}$$

and

$$|^2\Psi_u\rangle = \frac{\chi_A(1) - \chi_B(1)}{\sqrt{2}} \quad \text{(doublet } u\text{)} \tag{11}$$

In order to compute the cumulant Λ_{zz}, it is convenient to place the origin of the coordinates in the midpoint between A and B: in this way, the mean value of $\hat{Z}$ vanishes, and the only contribution comes from the mean value of $\hat{Z}^2$. Only the one-electron term contributes, and we obtain

$$\begin{aligned}\langle {}^2\Psi_g | \hat{Z}_m^{\,2} | {}^2\Psi_g \rangle &= \langle {}^2\Psi_u | \hat{Z}_m^{\,2} | {}^2\Psi_u \rangle \\ &= \frac{R^2}{4}\end{aligned} \tag{12}$$

We switch now to the neutral hydrogen molecule. Let us consider first the two neutral forms (a singlet and a triplet), $|^1\Psi_g\rangle$ and $|^3\Psi_u\rangle$, given by (again, only the spatial part is reported)

$$|^1\Psi_g\rangle = \frac{\chi_A(1)\chi_B(2) + \chi_B(1)\chi_A(2)}{\sqrt{2}} \quad \text{(singlet } g\text{)} \tag{13}$$

and

$$|^3\Psi_u\rangle = \frac{\chi_A(1)\chi_B(2) - \chi_B(1)\chi_A(2)}{\sqrt{2}} \quad \text{(triplet } u\text{)} \tag{14}$$

We have

$$\langle {}^1\Psi_g | \hat{Z}_m^{\,2} | {}^1\Psi_g \rangle = \langle {}^3\Psi_u | \hat{Z}_m^{\,2} | {}^3\Psi_u \rangle = \frac{R^2}{2} \tag{15}$$

while

$$\langle {}^1\Psi_g | \hat{Z}_b^{\,2} | {}^1\Psi_g \rangle = \langle {}^3\Psi_u | \hat{Z}_b^{\,2} | {}^3\Psi_u \rangle = -\frac{R^2}{2} \tag{16}$$

In both cases, the one-electron contribution is $R^2/2$, while the two-electron one is $-R^2/2$. This means that, for the two neutral states, the total value of $\mathbf{\Lambda}$ is equal to zero:

$$\langle {}^1\Psi_g | \hat{Z}^2 | {}^1\Psi_g \rangle = \langle {}^3\Psi_u | \hat{Z}^2 | {}^3\Psi_u \rangle = 0 \tag{17}$$

Let us consider now an ionic determinant. We can take, for instance, the determinant $|^1\Psi_A\rangle$, in which both electrons are located on the center A:

$$|^1\Psi_A\rangle = \chi_A(1)\chi_A(2) \quad \text{(singlet)} \tag{18}$$

In such a case, it is convenient to place the origin of the coordinates in A: the mean value of both $\hat{Z}$ and $\hat{Z}^2$ is zero and, again, Λ_{zz} vanishes.

If, however, a combination of two ionic determinants is considered, the situation is completely different. Let us take, for instance, the out-of-phase combination of the ionic distributions

$$|^1\Psi_A\rangle = \frac{\chi_A(1)\chi_A(2) - \chi_B(1)\chi_B(2)}{\sqrt{2}} \quad \text{(singlet } u\text{)} \tag{19}$$

By placing the coordinate origin in the midpoint between A and B, again the mean value of $\hat{Z}$ will vanishes by symmetry. The two contributions to $\hat{Z}^2$ are

$$\langle {}^1\Psi_u | \hat{Z}_m^{\,2} | {}^1\Psi_u \rangle = \left(-\frac{R}{2}\right)^2 + \left(\frac{R}{2}\right)^2 = \frac{R^2}{2} \tag{20}$$

while

$$\langle {}^1\Psi_u | \hat{Z}_b^{\,2} | {}^1\Psi_u \rangle = \left(-\frac{R}{2}\right)^2 + \left(\frac{R}{2}\right)^2 = \frac{R^2}{2} \tag{21}$$

and, therefore,

$$\langle {}^1\Psi_u | \hat{Z}^2 | {}^1\Psi_u \rangle = \frac{R^2}{2} + \frac{R^2}{2} = R^2 \tag{22}$$

The same result is obtained for the in-phase combination of the ionic distributions (an excited singlet state),

$$|2^1\Psi_g\rangle = \frac{\chi_A(1)\chi_A(2) + \chi_B(1)\chi_B(2)}{\sqrt{2}} \quad (\text{singlet } g) \tag{23}$$

which gives

$$\langle 2^1\Psi_g|\hat{Z}^2|2^1\Psi_g\rangle = \frac{R^2}{2} + \frac{R^2}{2} = R^2 \tag{24}$$

We consider now a slightly more-complex situation, where three determinants give a significant contribution to the (singlet) wave function. They are the ionic term $|^1\Psi_A\rangle$ and the neutral singlet $|^1\Psi_g\rangle$, mixed in variable proportions. Therefore, we write

$$\begin{aligned} |^1\Psi(\theta)\rangle &= \sin(\theta)|^1\Psi_A\rangle + \cos(\theta)|^1\Psi_g\rangle \\ &= \sin(\theta)\chi_A(1)\chi_A(2) \\ &\quad + \frac{\cos(\theta)\chi_A(1)\chi_B(2) + \chi_B(1)\chi_A(2)}{\sqrt{2}} \end{aligned} \tag{25}$$

In this case, again, it is convenient to place the coordinate origin in the midpoint between A and B. However, one must consider that, now, the contribution that comes from $\langle\hat{Z}\rangle$ will not vanish and must be taken into account. One has

$$\langle\hat{Z}_m^2\rangle = \sin^2(\theta)\frac{R^2}{2} + \cos^2(\theta)\frac{R^2}{2} \tag{26}$$

and

$$\langle\hat{Z}_b^2\rangle = \sin^2(\theta)\frac{R^2}{2} - \cos^2(\theta)\frac{R^2}{2} \tag{27}$$

and, hence,

$$\langle\hat{Z}^2\rangle = 2\sin^2(\theta)\frac{R^2}{2} = \sin^2(\theta)R^2 \tag{28}$$

On the other hand,

$$\langle\hat{Z}\rangle = -\sin^2(\theta)R \tag{29}$$

and, therefore,

$$\langle\hat{Z}\rangle^2 = \sin^4(\theta)R^2 \tag{30}$$

The cumulant $\Lambda_{||}$ as a function of θ becomes

$$\Lambda_{zz}(\theta) = R^2[\sin^2(\theta) - \sin^4(\theta)] = r^2\sin^2(\theta)\cos^2(\theta) \tag{31}$$

The cumulant is zero for $\theta = 0$ or $\theta = \pi/2$, while it reaches a maximum of $R^2/4$ for a value of $\theta = \pi/4$.

■ ASSOCIATED CONTENT

Supporting Information

Supporting figures showing the FCI potential energy curves of the ground state of the H_2, Li_2, N_2, F_2, BeH^-, He_2, HeH^-, and Be_2 molecules, the one-electron and two-electron terms of the TPS for the FCI ground state of H_2, and the longitudinal component of the TPS for the UHF wave function of H_2. This material is available free of charge via the Internet at http://pubs.acs.org.

■ AUTHOR INFORMATION

Corresponding Author

*E-mail: anc@unife.it.

Notes

The authors declare no competing financial interest.

■ ACKNOWLEDGMENTS

We thank the University of Toulouse and the French CNRS for financial support. M.E.K. acknowledges the ANR-DFG action ANR-11-INTB-1009 MITLOW for his Ph.D. grant. O.B. acknowledges the support of the Erasmus Mundus program of the European Union (FPA 2010-0147). C.A. has been financed by the Italian MIUR through its PRIN 2009 funds.

■ REFERENCES

(1) Kohn, W. *Phys. Rev.* **1964**, *133*, A171.
(2) Resta, R.; Sorella, S. *Phys. Rev. Lett.* **1999**, *82*, 370.
(3) Resta, R. *Phys. Rev. Lett.* **2005**, *95*, 196805.
(4) Resta, R. *Eur. Phys. J. B* **2011**, *79*, 121.
(5) Souza, I.; Wilkens, T.; Martin, R. M. *Phys. Rev. B* **2000**, *62*, 1666.
(6) Resta, R. *Phys. Rev. Lett.* **2006**, *96*, 137601.
(7) Resta, R. *J. Phys. Chem.* **2006**, *124*, 104104.
(8) Vetere, V.; Monari, A.; Bendazzoli, G. L.; Evangelisti, S.; Paulus, B. *J. Phys. Chem.* **2008**, *128*, 024701.
(9) Bendazzoli, G. L.; Evangelisti, S.; Monari, A.; Paulus, B.; Vetere, V. *J. Phys. Conf. Series* **2008**, *117*, 012005.
(10) Bendazzoli, G. L.; Evangelisti, S.; Monari, A. *Int. J. Quantum Chem.* **2011**, *111*, 3416.
(11) Angeli, C.; Bendazzoli, G. L.; Evangelisti, S. *J. Chem. Phys.* **2013**, *138*, 054314.
(12) Giner, E.; Bendazzoli, G. L.; Evangelisti, S.; Monari, A. *J. Chem. Phys.* **2013**, *138*, 074315.
(13) Monari, A.; Bendazzoli, G. L.; Evangelisti, S. *J. Chem. Phys.* **2008**, *129*, 134104.
(14) Bendazzoli, G. L.; Evangelisti, S.; Monari, A. *Theor. Chem. Acc.* **2010**, *126*, 257.
(15) Bendazzoli, G. L.; Evangelisti, S.; Monari, A.; Resta, R. *J. Chem. Phys.* **2010**, *133*, 064703.
(16) Bendazzoli, G. L.; Evangelisti, S.; Monari, A. *Int. J. Quantum Chem.* **2012**, *112*, 653.
(17) Monari, A.; Evangelisti, S. Finite size effects in graphene nanostructures. In *Physics and Applications of Graphene: Theory*; InTech Publishing: Wien, Austria, 2011; Chapter 14, pp 303−318.
(18) Ángyán, J. G. *Curr. Org. Chem.* **2011**, *15*, 3609.
(19) Ángyán, J. G. *Int. J. Quantum Chem.* **2009**, *109*, 2340.
(20) Widmark, P.-O.; Malmqvist, P.-Å.; Roos, B. O. *Theor. Chem. Acc.* **1990**, *77*, 291.
(21) *DALTON, a Molecular Electronic Structure Program, Release 2.0 (2005)*. See http://www.kjemi.uio.no/software/dalton/dalton.html (accessed October 5, 2013).
(22) Aidas, K.; Angeli, C.; Bak, K. L.; Bakken, V.; Bast, R.; Boman, L.; Christiansen, O.; Cimiraglia, R.; Coriani, S.; Dahle, P.; Dalskov, E. K.; Ekström, U.; Enevoldsen, T.; Eriksen, J. J.; Ettenhuber, P. Ferńandez, B.; Ferrighi, L.; Fliegl, H.; Frediani, L.; Hald, K.; Halkier, A.; Hättig, C.; Heiberg, H.; Helgaker, T.; Hennum, A. C.; Hettema, H.; Hjertenæs, E.; Høst, S.; Høyvik, I.-M.; Iozzi, M. F.; Jańsık, B.; Jensen, H. J. A.; Jonsson, D.; Jørgensen, P.; Kauczor, J.; Kirpekar, S.; Kjærgaard, T.; Klopper,W.; Knecht, S.; Kobayashi, R.; Koch, H.; Kongsted, J.; Krapp, A.; Kristensen, K.; Ligabue, A.; Lutnæs, O. B.; Melo, J. I.; Mikkelsen, K. V.; Myhre, R. H.; Neiss, C.; Nielsen, C. B.; Norman, P.; Olsen, J.; Olsen, J. M. H.; Osted, A.; Packer, M. J.; Pawlowski, F.; Pedersen, T. B.; Provasi, P. F.; Reine, S.; Rinkevicius, Z.; Ruden, T. A.; Ruud, K.; Rybkin, V. V.; Sałek, P.; Samson, C. C. M.; Śanchez de Meŕas, A.; Saue, T.; Sauer, S. P. A.; Schimmelpfennig, B.; Sneskov, K.; Steindal, A. H.; Sylvester-Hvid, K. O.; Taylor, P.; Teale, A. M.; Tellgren, E. I.; Tew, D. P.; Thorvaldsen, A. J.; Thøgersen, L.; Vahtras, O.; Watson, M. A.; Wilson, D. J. D.; Ziolkowski, M.; Ågren, H. *WIREs Comput. Mol. Sci.* in press, DOI: 10.1002/wcms.1172.
(23) Cimiraglia, R. Private communication.
(24) Bendazzoli, G. L.; Evangelisti, S. *J. Chem. Phys.* **1993**, *98*, 3141.

(25) Bendazzoli, G. L.; Evangelisti, S. *Int. J. Quantum Chem.* **1993**, *27*, 287.
(26) Gagliardi, L.; Bendazzoli, G. L.; Evangelisti, S. *J. Comput. Chem.* **1997**, *18*, 1329.
(27) Bendazzoli, G. L.; Evangelisti, S. NEPTUNUS, a Full CI program written by G. L. Bendazzoli and S. Evangelisti, with contributions by A. Monari, L. Gagliardi.
(28) Angeli, C.; Bendazzoli, G. L.; Borini, S.; Cirmiraglia, R.; Emerson, A.; Evangelisti, S.; Maynau, D.; Monari, A.; Rossi, E.; Sanchez-Marìn, J.; Szalay, P.; Tajti, A. *Int. J. Quantum Chem.* **2007**, *107*, 2082.
(29) Borini, S.; Monari, A.; Rossi, E.; Tajti, A.; Angeli, C.; Bendazzoli, G. L.; Cirmiraglia, R.; Emerson, A.; Evangelisti, S.; Maynau, D.; Sanchez-Marìn, J.; Szalay, P. *J. Chem. Inf. Model.* **2007**, *47*, 1271.
(30) Rampino, S.; Monari, A.; Evangelisti, S.; Rossi, E.; Laganà, A. *Chem. Phys.* **2012**, *47*, 192.
(31) Angeli, C.; Cimiraglia, R.; Malrieu, J.-P. *J. Chem. Educ.* **2008**, *85*, 150.
(32) Shaik, S.; Danovich, D.; Silvi, B.; Lauvergnat, D. L.; Hiberty, P. C. *Chem.—Eur. J.* **2005**, *11*, 6358.
(33) Hiberty, P. C.; Ramozzi, R.; Song, L.; Wu, W.; Shaik, S. *Faraday Discuss.* **2007**, *135*, 261.
(34) Persico, M. Electronic diabatic states: definition, computation, and applications. In *Encyclopedia of Computational Chemistry*, Vol. 2; John Wiley and Sons: Chichester, U.K., 2010; p 852.
(35) Angeli, C.; Cimiraglia, R.; Malrieu, J.-P. *Mol. Phys.* **2013**, *111*, 1069.
(36) Bauschlicher, C. W.; Langhoff, S. R. *J. Chem. Phys.* **1988**, *89*, 4246.
(37) Bendazzoli, G. L.; Evangelisti, S.; Passarini, F. *Chem. Phys.* **1997**, *215*, 217.
(38) Verdicchio, M.; Bendazzoli, G. L.; Evangelisti, S.; Leininger, T. *J. Phys. Chem. A* **2013**, *117*, 192.
(39) Knowles, P.; Werner, H. J. *Molpro Quantum Chemistry Package*; available via the Internet at http://www.molpro.net (accessed October 5, 2013).
(40) Schaad, L. *J. Chem. Phys.* **1970**, *53*, 851.
(41) Bishop, D. M.; Wetmore, R. W. *Mol. Phys.* **1973**, *26*, 145.
(42) Kołos, W.; Wolniewicz, L. *J. Chem. Phys.* **1965**, *43*, 2429.
(43) Velasco, R.; Ottinger, C.; Zare, R. N. *J. Chem. Phys.* **1969**, *51*, 5522.
(44) Christian, R. H.; Duff, R. E.; Yarger, F. L. *J. Chem. Phys.* **1955**, *23*, 2045.
(45) DeCorpo, J. J.; Steiger, R. P.; Franklin, J. L. *J. Chem. Phys.* **1970**, *53*, 936.
(46) Brazier, C. R.; Oliphant, N. H.; Bernath, P. F. *Chem. Rev.* **1961**, *61*, 425.
(47) Ogilvie, J. F.; Wang, F. Y. H. *J. Mol. Struct.* **1992**, *273*, 277.
(48) Li, Y.; Lin, C. *Phys. Rev. A* **1999**, *60*, 2009.
(49) Bondybey, V. E.; English, J. H. *J. Chem. Phys.* **1984**, *80*, 568.
(50) Kenney, J.; Simons, J. *J. Chem. Phys.* **1975**, *62*, 592.